HHS Public Access

Author manuscript

Phys Med Biol. Author manuscript; available in PMC 2018 April 21.

Published in final edited form as:

Phys Med Biol. 2017 April 21; 62(8): 3111–3123. doi:10.1088/1361-6560/aa6024.

Fast Lesion Mapping during HIFU Treatment Using Harmonic Motion Imaging guided Focused Ultrasound (HMIgFUS) *In Vitro* and *In Vivo*

Yang Han[1], **Shutao Wang**[1], **Thomas Payen**[1], and **Elisa Konofagou**[1,2]

[1]Department of Biomedical Engineering, Columbia University, New York, NY, USA

[2]Department of Radiology, Columbia University, New York, NY, USA

Abstract

The successful clinical application of High Intensity Focused Ultrasound (HIFU) ablation depends on reliable monitoring of the lesion formation. Harmonic Motion Imaging guided Focused Ultrasound (HMIgFUS) is an ultrasound-based elasticity imaging technique, which monitors HIFU ablation based on the stiffness change of the tissue instead of the echo intensity change in conventional B-mode monitoring, rendering it potentially more sensitive to lesion development. Our group has shown that predicting the lesion location based on the radiation force-excited region is feasible during HMIgFUS. In this study, the feasibility of a fast lesion mapping method is explored to directly monitor the lesion map during HIFU. The HMI lesion map was generated by subtracting the reference HMI image from the present HMI peak-to-peak displacement map to be streamed on the computer display. The dimensions of the HMIgFUS lesions were compared against gross pathology. Excellent agreement was found between the lesion depth (r^2 = 0.81, slope = 0.90), width (r^2 = 0.85, slope = 1.12) and area (r^2 = 0.58, slope = 0.75). *In vivo* feasibility was assessed in a mouse with a pancreatic tumor. These findings demonstrate that HMIgFUS can successfully map thermal lesion and monitor lesion development in real time *in vitro* and *in vivo*. The HMIgFUS technique may therefore constitute a novel clinical tool for HIFU treatment monitoring.

Keywords

HMI; HMIgFUS; lesion quantification; fast lesion mapping; real-time HIFU monitoring

Introduction

High intensity focused ultrasound (HIFU) ablation is a noninvasive treatment procedure, which delivers a large amount of energy to cause localized temperature rise and cell necrosis. Numerous studies and clinical trials have used HIFU to treat local diseases in organs such as the thyroid, prostate, breast, pancreas and liver (Esnault *et al* 2011, Warmuth

Address correspondence to: Dr. Elisa Konofagou, Department of Biomedical Engineering, Columbia University, 351 Engineering Terrace, mail code 8904, 1210 Amsterdam Avenue, New York, NY, USA, ek2191@columbia.edu, Tel: 212-342-0863.

et al 2010, Peek *et al* 2015, Jang *et al* 2010, Wijlemans *et al* 2012). The clinical translation and accessibility of HIFU relies heavily on improving its treatment monitoring.

There are several techniques currently being investigated to detect real-time treatment performance of HIFU. Magnetic resonance imaging (MRI) thermometry (Dibaji et al. 2014; McDannold et al. 2000) is used to detect temperature rise across the treatment area. However, MRI guidance can be expensive and time consuming compared to ultrasound-based HIFU guidance; the temporal resolution for this clinical applications is usually between 2 and 6 s (Wijlemans *et al* 2012). Among the ultrasound guidance techniques, conventional B-mode-based 'hyperecho' tracking is not robust for HIFU monitoring as it is sensitive to air bubbles, which occur at high temperatures and usually lead to over-treatment of the targeted region (Yu and Xu 2008, Ueno *et al* 1990). Passive acoustic mapping (PAM) has also been investigated regarding it capability of monitoring HIFU ablation by reconstructing the emissions generated by inertially cavitating bubbles during HIFU. However, the estimates of cavitation location and intensity are also prone to errors due to the limited axial resolution (Jensen *et al* 2012, 2013).

Over the past two decades, ultrasound elasticity imaging has expanded from diagnostic technique to include therapy guidance and monitoring based on tissue stiffness change (Souchon *et al* 2003, Thittai *et al* 2011, Kwiecinski *et al* 2015). Compared to bubble- or cavitation-based methods, elasticity imaging does not rely on, or is affected by, boiling air bubbles formed at the focus but monitors the change in the tissue characteristics. However, most elasticity imaging techniques require HIFU to be interrupted for reliable monitoring, and therefore cannot detect the onset of lesion formation in real time, significantly increasing the treatment duration and cumulatively reduces the efficiency of a HIFU treatment.

Harmonic Motion Imaging (HMI) is a radiation-force-based ultrasound elasticity imaging technique which is designed for both tissue relative stiffness imaging and reliable HIFU treatment monitoring. An amplitude-modulated (AM) HIFU beam is transmitted through a focused ultrasound (FUS) transducer to induce tissue vibration at the focal region. The oscillatory response from the tissue can be tracked using radio-frequency (RF) signals acquired with a confocally-aligned imaging transducer (Konofagou and Hynynen 2003, Maleke and Konofagou 2008). The oscillatory displacement amplitude, namely HMI displacement, is monitored continuously to provide real-time tissue stiffness change during the treatment. Without interrupting the ablative procedure, Harmonic Motion Imaging guided Focused Ultrasound (HMIgFUS) can be applied with optimal efficiency to the targeted area. Several studies have been published showing feasibility of HMI on post-surgical human breast tissue (Han *et al* 2016), *ex vivo* canine liver (Hou *et al* 2014b, Han *et al* 2015) and *in vivo* mice (Payen *et al* 2016, Chen *et al* 2015). A fast imaging and processing algorithm is essential to ensure real-time lesion mapping. Recently, HMI was shown capable of streaming HMI displacement in real time at 15 frames per second (Grondin *et al* 2015). Although the oscillatory HMI displacement contains important information on tissue stiffness change, it does not provide information on the lesion location or lesion size itself in real time. A fast lesion mapping method that can inform physicians

intuitively on the progression of thermal lesioning in real time without sacrificing the frame rate is thus wanted.

Our objective in this study is first to develop a HMIgFUS-based lesion quantification method to map and quantify HIFU-induced thermal lesions. We also aimed at demonstrating the accuracy as well as reproducibility of the lesion quantification method through gross pathology validation *in vitro* and *in vivo*. Finally, we aimed at implementing a fast lesion mapping method for online processing to achieve lesion formation monitoring during HMIgFUS treatment in real time.

Methods and materials

I. HMI

In HMI, the radiation force generated at the focal region can be expressed with equation (1) with the assumption of attenuating homogenous medium and linear plane wave propagation (Torr 1984, Starritt *et al* 1991):

$$F=\frac{2\alpha I}{c} \quad (1)$$

where F is the radiation force generated [N/m^3], α is the tissue absorption coefficient [m^{-1}], I is the temporal average acoustic intensity [W/m^2] and c is the sound speed[m/s]. With AM at the frequency ω_m on the HIFU beam, an oscillatory radiation force is generated at the focal region to vibrate the tissue at ω_m, which is 100 Hz in this study. The oscillatory displacement is monitored continuously through a phased array imaging transducer. The changes in estimated displacement amplitude can be used to indicate the relative stiffness change when the lesion is starting to form at the focal region.

II. HMIgFUS

Fig. 1 shows an illustration of the experiment setup. The HMIgFUS system consisted of a FUS transducer and a phased array imaging probe coaligned through the central opening (diameter = 41 mm) of the FUS transducer. The FUS transducer was a 93-element phased array (f_c = 4.5 MHz, and D = 70 mm, Sonic Concepts Inc., Bothell WA, USA). And the imaging probe was a 64-element phased array (f_c = 2.5 MHz, P4-2, ATL/Philips, Bothell, WA, USA). A dual-channel arbitrary waveform generator (AT33522A, Agilent Technologies Inc. Santa Clara, CA, USA) was used to generate an AM sinusoidal signal to drive the FUS transducer through a 50-dB power amplifier (325LA, E&I, Rochester, NY, USA). The imaging probe was inserted through the central opening and confocally aligned with the FUS transducer. The imaging probe was transmitting and receive through an ultrasound imaging research system (Vantage, Verasonics, Bothell, WA, USA) with a pulse repetition frequency (prf) at 1000 Hz. The FUS total output acoustic power was within the range of 6.4 – 8.6 W from radiation force balance measurements (Hynynen 2011). A T-type bare wire thermocouple with a diameter of 80 μm (Physitemp Instruments Inc., Clifton, NJ, USA) was inserted into the tissue and aligned with the focal spot for temperature monitoring at the focal region.

III. Real-time HMIgFUS and displacement estimation

During real-time HMIgFUS, the RF channel data was acquired at a prf of 1000 frames/s. In order to calculate the peak-to-peak HMI displacement without sacrificing the display frame rate, only 10 consecutive frames within a single HMI vibration were obtained at each acquisition and transferred to a host computer. The RF channel data matrix was placed into a GPU matrix within Matlab and multiplied by a beamforming sparse matrix to get the beamformed RF data (Hou *et al* 2014a, Grondin *et al* 2015). A 1D cross-correlation method (Luo and Konofagou 2010) was used to estimate the incremental axial displacement between 2 consecutive RF frames. HMI peak-to-peak displacement maps were calculated over each of the 10 frames of HMI displacement maps by subtracting the minimum displacement from the maximum displacement on each pixel. When the processing is finished, another 10 frames will be acquired for processing. The peak-to-peak HMI displacement map averaged over the first 1s of treatment served as a reference map. The HMI lesion map was generated by subtracting the reference HMI image from the current HMI peak-to-peak displacement map to be displayed on computer screen (Fig. 2).

IV. Materials

In vitro canine liver specimens—6 *in vitro* canine liver specimens were used for this study as they are relatively homogeneous, allowing easy optical delineation of the lesions in gross pathology. Liver specimens were prepared and degassed for 2 hours before each experiment. After ablation, each liver specimen was carefully sectioned at the imaging plane under the guidance of B-mode for gross pathology. The lesion area was delineated based on the color change in tissue. The depth, width and area of the lesions measured on gross pathology were compared with HMI lesion mapping. We tested 0 dB, −1.5 dB, −3 dB and −6 dB thresholding. We then chose to set a −3 dB or 30% displacement decrease as the threshold to discriminate the ablated from unablated tissue as it yields the best correlation with gross pathology. The largest region closest to the geometric focus was identified as the lesion.

In vivo pancreatic tumor mouse experiment—The animal experiment protocol was approved by the Institutional Animal Care and Use Committee (IACUC) of the Columbia University. The transgenic mouse model (K-$^{rasLSL.G12D/+}$; p53$^{R172H/+}$; PdxCre (KPC)) (Olive and Tuveson 2006, Olive *et al* 2010) was used to develop pancreatic tumor which is pathophysiologically resembling human pancreatic ductal adenocarcinoma (PDA). One KPC mouse was used for this study. The mouse was laying supine under isoflurane anesthesia with it abdomen shaved and covered with ultrasound gel, with a degassed water tank on top to be coupled for ultrasound imaging. To precisely locate the pancreas, an 18.5-MHz diagnostic probe (L22-14v, Verasonics, Bothell, WA, USA) was used in the planning stage providing high resolution B-mode images to locate and differentiate organs. By aligning the HMI imaging plane with the high resolution B-mode images, the HMI images are spatially registered with the B-mode images. In the treatment monitoring stage, the center imaging probe of HMIgFUS was replaced with a 104-element phased array (f_c = 7.8 MHz, P12-5, ATL/Philips, Bothell, WA, USA) for higher resolution more adapted to small animals. The treatment power on the tumor was 6.4 W with 60 s duration.

The mouse was immediately sacrificed after the previously described procedure. Because gross pathology was incapable of distinguishing the ablated lesion from the pancreatic tumor, the whole pancreas along with the tumor was harvested for histological evaluation. The excised tissue was first fixed in 4% paraformaldehyde. After post-fixation processing, tissue was embedded in paraffin, sectioned, and stained with hematoxylin and eosin (H&E). Bright field microscopy images were acquired and evaluated by a trained expert.

Results

A. Real-time HMIgFUS ablation monitoring

The fast lesion mapping of HMIgFUS can stream the HMI displacement, HMI displacement overlaid on B-mode and HMI lesion map to the computer screen (Fig. 3) at an average frame rate of 2.4 Hz. In the HMI displacement map, positive displacement is towards the transducer and negative displacement is away from the transducer.

B. In vitro liver results

In order to prove the reproducibility of the technique, we have generated 13 lesions with HMIgFUS using different acoustic powers (6.4 W and 8.6 W) with different treatment duration varies from 90s to 120s. The lesions were detected and visualized at 2.4 Hz.

Figure 4 shows a representative case of HMIgFUS lesion monitoring over 90s ablation. Yellow indicates HMI peak-to-peak displacement amplitude increase (softening) and blue indicates HMI peak-to-peak displacement amplitude decrease (stiffening). No lesioning was found by HMI until 50s into the treatment when a dark blue spot was detected at the focal spot region (Fig. 4(a)) indicating tissue stiffening. The lesion was found to grow during ablation, which is also quantified in Fig. 4(d) showing that the lesion size increased after 50s. When temperature rises above a certain threshold, liver tissue undergoes irreversible stiffening change, which is caused by protein denaturation. According to established studies (Hill *et al* 1994, Hynynen 1996, Righetti *et al* 1999), 58–60°C is the conventional “threshold” for the formation of HIFU lesions in the liver. The temporal temperature profile (Fig. 4(e)) was obtained showing the temperature at the focal spot reaching the threshold of 60°C at 30s (denoted with red line). Normalized HMI displacement within the focal region (Han *et al* 2015) was plotted against the temperature clearly showing the displacement change with temperature increase. A gross pathological cross section of the lesion was shown in Fig. 4(b) for comparison with the final HMI lesion map Fig. 4(c).

Figure 5 is another representative case of 120s HMIgFUS lesion monitoring. Lesioning was detected by HMI after 40s of sonication with a decrease in displacement at the focal spot indicating tissue stiffening (Fig. 5(a)). Lesion growth during ablation is also quantified in Fig. 5(d) showing that the lesion size increased after 50s. The temperature profile over time (Fig. 5(e)) showed that the temperature at the focal spot reached the 60°C threshold at 30s (denoted with red line). Normalized HMI displacement within the focal region was also plotted against temperature clearly showing the displacement change with temperature. A gross pathological cross-section of the lesion was shown in Fig. 5(b) in comparison with the HMI final lesion map Fig. 5(c).

Statistical analysis was performed with linear regression in 13 HMIgFUS-induced lesions to compare the lesion dimension identified with HMI and gross pathology. The R^2 value from the linear regression analysis equal to 0.81 and 0.85 in depth and width. The linear regression performed in the lesion area gives a R^2 equals to 0.75 (Fig. 6).

C. Multiple-lesion results

In HIFU clinical applications, multiple-lesion ablations are often needed to treat the entire target region. When a few lesions come close together, the lesions generated later start to merge into those created before. An example of a three-lesion HMIgFUS case was shown in Fig. 7. The three lesions are 3 mm apart at the same ablation power and duration starting from location 1 and then moving towards the right to locations 2 and 3 (Fig. 7(a)). Same lesion quantification protocol was used in each location. After combining lesion maps from 3 locations, a final combined HMI lesion map was obtained in Fig. 7(d).

C. In vivo tumor results

HMIgFUS lesion maps within the tumor area at the beginning (t = 3s) and the end (t = 59s) of the ablation are shown in Fig. 8(a–b). The pancreatic tumor was delineated based on the high-resolution B-mode images. In Fig. 8(a), the lesion map within the tumor was homogeneous and no lesion was indicated at the onset of ablation. Fig. 8(b) exhibits stiffening within the tumor after a 59s-ablation with a displacement reduction rate of 43.3%, suggesting lesion formation. The H&E staining results in Fig. 8(c) confirmed that thermal lesion was generated in the tumor with apparent hemorrhage and tissue disruption.

Discussion

In the field of MRI and ultrasound imaging, numerous guidance techniques have been developed for the 3 stages of HIFU treatment: planning, monitoring and assessment. Although numerous methods have been developed to assist the 3 stages of HIFU treatment, real-time HIFU monitoring still remain as a challenge. Real-time HIFU monitoring, especially lesion mapping, is essential during HIFU procedure as it can help avoid any over- or under-treatment. HMIgFUS is capable of performing HIFU monitoring based on the stiffness change of the tissue without interrupting treatment. Throughout this study, we developed a lesion quantification method using HMIgFUS, and investigated the feasibility of real-time lesion formation monitoring, which incorporated a GPU-based, fast beamforming method. The lesion quantification method was validated through *in vitro* experiments in liver and showed promising results *in vivo*.

In addition to lesion stiffening, softening was also detected at the focal spot when temperature is within the range of 40–60°C before the lesion started to form (Fig. 4(a) at 30s). This agreed with previous literature on liver showing a slow, reversible shear modulus decrease under HIFU treatment before reaching the threshold of irreversible protein denaturation (Wu *et al* 2001). At the end of treatment, softening is also detected around the lesion boundary area in most cases indicating heat diffusion to adjacent region. We found that heat diffusion after HIFU is turned off will not affect the lesion size significantly by comparing it with another lesion map acquired 5 min after ablation. According to the

temperature profile obtained by the thermocouple, temperature measured from the focal spot drops back to room temperature rapidly within 1 min after HIFU is turned off. A post-treatment HMI was performed 5 min after HIFU exposure showing the lesion dimensions remain the same. Therefore, the lesion map at the end of HMIgFUS can represent the final lesion. Since the speed of sound change is filtered out from the displacement map (Maleke and Konofagou 2008), the effect of speed of sound change due to temperature increase can also be excluded. Furthermore, the increase in attenuation can occur during thermal lesioning (Zderic *et al* 2004), resulting in increased absorption therefore increased radiation force within the stiffer lesioning area. However, it has been shown that the decrease in displacement amplitude occurs approximately after reaching 60°C due to the combined effect of viscoelasticity changes and lesion growth overpowering the effect of attenuation (Suomi *et al* 2016, Hou *et al* 2015). The increased radiation force during ablation may generate an opposite lesion-to-background contrast by generating higher HMI displacement inside the lesion, which was not observed in this study. It is therefore concluded that the stiffening process is dominant over the change of absorption coefficient in HIFU ablation in liver.

Despite our successful implementation on real-time HMIgFUS platforms, one limitation was that there was no absolute threshold of relative stiffness change to distinguish ablated liver tissue. However, the displacement change during and after treatment has shown enough contrast to delineate the HIFU lesion. −3 dB or 30% decrease out of 0 dB, −1.5 dB and −6 dB showed the best agreement with the gross pathology. This can be improved by optimization study, which can adapt the lesion threshold for each specific specimen. The lesion size was not quantifiable on H&E staining for 2 reasons: 1) it was difficult to register the imaging plane with the cutting plane in histology due to the harvest process; 2) soft tissue shrinks in the paraformaldehyde fixing process, which makes the lesion size smaller when compare with the actual lesion size in vivo. A registration method will be used in the future to register the orientation of the lesion with the help of surrounding organs. Another limitation of this study lies in the fact that only slow denaturation induced ablation was included in the study. However, previous work (Hou *et al* 2015) from our group has shown that HMIgFUS is robust under faster treatments such as boiling in monitoring the lesion formation in the presence of strong cavitation events with good displacement contrast across the entire treatment window. The present study may have the potential to be applied on cavitation induced HIFU treatment in the future.

As a final point, HMIgFUS combines HIFU and real-time elasticity imaging on the same device with the advantage of lesion formation monitoring without interfering HIFU treatment. Future studies will consider the correlation between tissue structures and HMI characteristics to better understand tissue mechanical responses during HMIgFUS ablation.

Conclusion

A real-time (2.4 Hz) lesion detection and ablation monitoring method was developed using oscillatory radiation force induced displacement amplitude variations in real time. Lesion size monitoring was achieved in canine liver *in vitro* and initial *in vivo* feasibility was shown in a mouse pancreatic tumor model. Using this method, the HMIgFUS focal region and

lesion formation were visualized in real time at a feedback rate of 2.4 Hz. By comparing the estimated lesion size against gross pathology, we have shown the feasibility of using HMIgFUS to monitor treatment and lesion formation without interruption. The study presented herewith validated that HMIgFUS could map lesion formation during HIFU treatment and capable of real-time HIFU monitoring.

Acknowledgments

This study was supported by the National Institutes of Health (R01EB014496). The authors thank K. P. Olive, Ph.D., and C. F. Palermo, Herbert Irving Comprehensive Cancer Center, Columbia University, for providing the mouse with pancreatic tumor.

References

Chen H, Hou G, Han Y, Payen T, Palermo C, Olive K, Konofagou E. Harmonic motion imaging in abdominal tumor detection and HIFU ablation monitoring: A feasibility study in a transgenic mouse model of pancreatic cancer. IEEE Trans Ultrason Ferroelectr Freq Control. 2015; 62:923–6.

Dibaji S, Wansapura J, Myers MR, Banerjee RK. In Vivo Monitoring of HIFU Induced Temperature Rise in Porcine Liver Using Magnetic Resonance Thermometry1. J Med Device. 2014; 8:30937.

Esnault O, Franc B, Ménégaux F, Rouxel A, De Kerviler E, Bourrier P, Lacoste F, Chapelon J-Y, Leenhardt L. High-Intensity Focused Ultrasound Ablation of Thyroid Nodules: First Human Feasibility Study. Thyroid. 2011; 21:965–73. [PubMed: 21834683]

Grondin J, Wang S, Payen de la Garanderie T, Konofagou E. Real-time monitoring of high intensity focused ultrasound (HIFU) ablation of in vitro canine livers using Harmonic Motion Imaging for Focused Ultrasound (HMIFU). J Vis Exp. 2015

Han Y, Hou GY, Wang S, Konofagou E. High intensity focused ultrasound (HIFU) focal spot localization using harmonic motion imaging (HMI). Phys Med Biol. 2015; 60:5911–24. [PubMed: 26184846]

Han Y, Wang S, Hibshoosh H, Taback B, Konofagou E. Tumor characterization and treatment monitoring of postsurgical human breast specimens using harmonic motion imaging (HMI). Breast Cancer Res. 2016; 18:46. [PubMed: 27160778]

Hill CR, Rivens I, Vaughan MG, ter Haar GR. Lesion development in focused ultrasound surgery: a general model. Ultrasound Med Biol. 1994; 20:259–69. [PubMed: 8059487]

Hou G, Provost J, Grondin J, Wang S, Marquet F, Bunting E, Konofagou E. Sparse matrix beamforming and image reconstruction for real-time 2D HIFU monitoring using Harmonic Motion Imaging for Focused Ultrasound (HMIFU) with in vitro validation. IEEE Trans Med Imaging. 2014a; 33:2107–17. [PubMed: 24960528]

Hou GY, Marquet F, Wang S, Apostolakis I, Konofagou EE. High-intensity focused ultrasound monitoring using harmonic motion imaging for focused ultrasound (HMIFU) under boiling or slow denaturation conditions. IEEE Trans Ultrason Ferroelectr Freq Control. 2015; 62:1308–19. [PubMed: 26168177]

Hou GY, Marquet F, Wang S, Konofagou EE. Multi-parametric monitoring and assessment of high-intensity focused ultrasound (HIFU) boiling by harmonic motion imaging for focused ultrasound (HMIFU): an ex vivo feasibility study. Phys Med Biol. 2014b; 59:1121–45. [PubMed: 24556974]

Hynynen K. Acoustic power calibrations of cylindrical intracavitary ultrasound hyperthermia applicators. Med Phys. 2011; 20:129–34.

Hynynen K. Focused Ultrasound Surgery Guided by MRI. Sci Med (Phila). 1996; 3:62–71.

Jang HJ, Lee J-Y, Lee D-H, Kim W-H, Hwang JH. Current and Future Clinical Applications of High-Intensity Focused Ultrasound (HIFU) for Pancreatic Cancer. Gut Liver. 2010; 4(Suppl 1):S57–61. [PubMed: 21103296]

Jensen CR, Cleveland RO, Coussios CC. Real-time temperature estimation and monitoring of HIFU ablation through a combined modeling and passive acoustic mapping approach. Phys Med Biol. 2013; 58:5833–50. [PubMed: 23920089]

Jensen CR, Ritchie RW, Collin JRT, Leslie T. Spatiotemporal Monitoring of High-Intensity Focused Ultrasound Therapy with Passive Acoustic Mapping. Radiology. 2012:262. [PubMed: 22025733]

Konofagou EE, Hynynen K. Localized harmonic motion imaging: theory, simulations and experiments. Ultrasound Med Biol. 2003; 29:1405–13. [PubMed: 14597337]

Kwiecinski W, Bessière F, Colas EC, Apoutou N'Djin W, Tanter M, Lafon C, Pernot M. Cardiac shear-wave elastography using a transesophageal transducer: application to the mapping of thermal lesions in ultrasound transesophageal cardiac ablation. Phys Med Biol. 2015; 60:7829–46. [PubMed: 26406354]

Luo J, Konofagou E. A fast normalized cross-correlation calculation method for motion estimation. IEEE Trans Ultrason Ferroelectr Freq Control. 2010; 57:1347–57. [PubMed: 20529710]

Maleke C, Konofagou EE. Harmonic motion imaging for focused ultrasound (HMIFU): a fully integrated technique for sonication and monitoring of thermal ablation in tissues. Phys Med Biol. 2008; 53:1773–93. [PubMed: 18367802]

McDannold NJ, King RL, Jolesz Fa, Hynynen KH. Usefulness of MR imaging-derived thermometry and dosimetry in determining the threshold for tissue damage induced by thermal surgery in rabbits. Radiology. 2000; 216:517–23. [PubMed: 10924580]

Olive KP, Jacobetz Ma, Davidson CJ, Mcintyre D, Honess D, Madhu B, Mae A, Caldwell ME, Allard D, Frese KK, Feig C, Combs C, Winter SP, Ireland H, Reichelt S, Howat WJ, Chang A, Dhara M, Wang L, Grützmann R, Pilarsky C, Izeradjene K, Hingorani SR, Huang P, Davies SE, Plunkett W, Egorin M, Hruban RH, Whitebread N, Mcgovern K, Adams J, Iacobuzio-donahue C. Inhibition of Hedgehog Signaling Enhances Delivery of Chemotherapy in a Mouse Model of Pancreatic Cancer. Cancer Res. 2010; 324:1457–61.

Olive KP, Tuveson DA. The use of targeted mouse models for preclinical testing of novel cancer therapeutics. Clin Cancer Res. 2006; 12:5277–87. [PubMed: 17000660]

Payen T, Palermo CF, Sastra SA, Chen H, Han Y, Olive KP, Konofagou EE. Elasticity mapping of murine abdominal organs in vivo using harmonic motion imaging (HMI). Phys Med Biol. 2016; 61:5741–54. [PubMed: 27401609]

Peek MCL, Ahmed M, Napoli A, ten Haken B, McWilliams S, Usiskin SI, Pinder SE, van Hemelrijck M, Douek M. Systematic review of high-intensity focused ultrasound ablation in the treatment of breast cancer. Br J Surg. 2015; 102:873–82. [PubMed: 26095255]

Righetti R, Kallel F, Stafford RJ, Price RE, Krouskop TA, Hazle JD, Ophir J. Elastographic characterization of HIFU-induced lesions in canine livers. Ultrasound Med Biol. 1999; 25:1099–113. [PubMed: 10574342]

Souchon R, Rouvière O, Gelet A, Detti V, Srinivasan S, Ophir J, Chapelon JY. Visualisation of HIFU lesions using elastography of the human prostate in vivo: Preliminary results. Ultrasound Med Biol. 2003; 29:1007–15. [PubMed: 12878247]

Starritt HC, Duck FA, Humphrey VF. Forces acting in the direction of propagation in pulsed ultrasound fields. Phys Med Bid. 1991; 36:1465–74.

Suomi V, Han Y, Konofagou E, Cleveland RO. The effect of temperature dependent tissue parameters on acoustic radiation force induced displacements. Phys Med Biol. 2016; 61:7427–47. [PubMed: 27694703]

Thittai AK, Galaz B, Ophir J. Visualization of HIFU-Induced lesion boundaries by axial-shear strain elastography: A feasibility study. Ultrasound Med Biol. 2011; 37:426–33. [PubMed: 21276656]

Torr GR. The acoustic radiation force. Am J Phys. 1984; 52:402.

Ueno, S., Hashimoto, M., Fukukita, H., Yano, T. Ultrasound thermometry in hyperthermia. Ultrason. Symp. 1990. Proceedings., IEEE 1990; 1990. p. 1645-52.

Warmuth M, Johansson T, Mad P. Systematic review of the efficacy and safety of high-intensity focussed ultrasound for the primary and salvage treatment of prostate cancer. Eur Urol. 2010; 58:803–15. [PubMed: 20864250]

Wijlemans JW, Bartels LW, Deckers R, Ries M, Mali WPTM, Moonen CTW, Van Den Bosch MAAJ. Magnetic resonance-guided high-intensity focused ultrasound (MR-HIFU) ablation of liver tumours. Cancer Imaging. 2012; 12:387–94. [PubMed: 23022541]

Wu T, Felmlee JP, Greenleaf JF, Riederer SJ, Ehman RL. Assessment of thermal tissue ablation with MR elastography. Magn Reson Med. 2001; 45:80–7. [PubMed: 11146489]

Yu T, Xu C. Hyperecho as the Indicator of Tissue Necrosis During Microbubble-Assisted High Intensity Focused Ultrasound: Sensitivity, Specificity and Predictive Value. Ultrasound Med Biol. 2008; 34:1343–7. [PubMed: 18378378]

Zderic V, Keshavarzi A, Andrew MA, Vaezy S, Martin RW. Attenuation of porcine tissues in vivo after high-intensity ultrasound treatment. Ultrasound Med Biol. 2004; 30:61–6. [PubMed: 14962609]

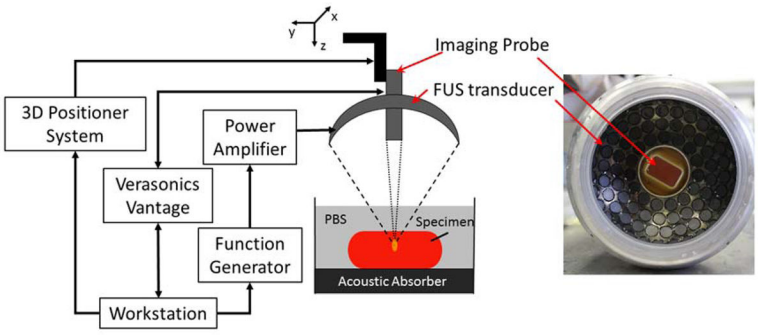

Figure 1.
HMIgFUS experimental setup and transducers.

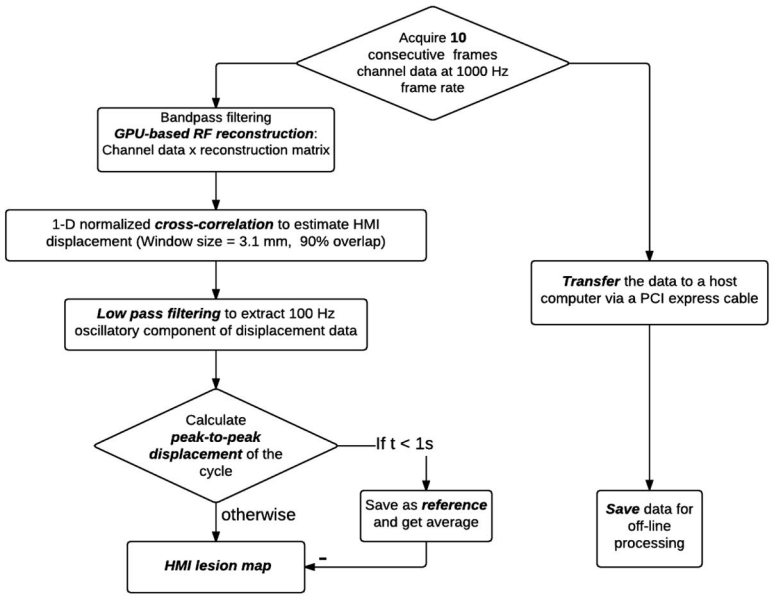

Figure 2.
Flowchart of real-time HMI reconstruction algorithm.

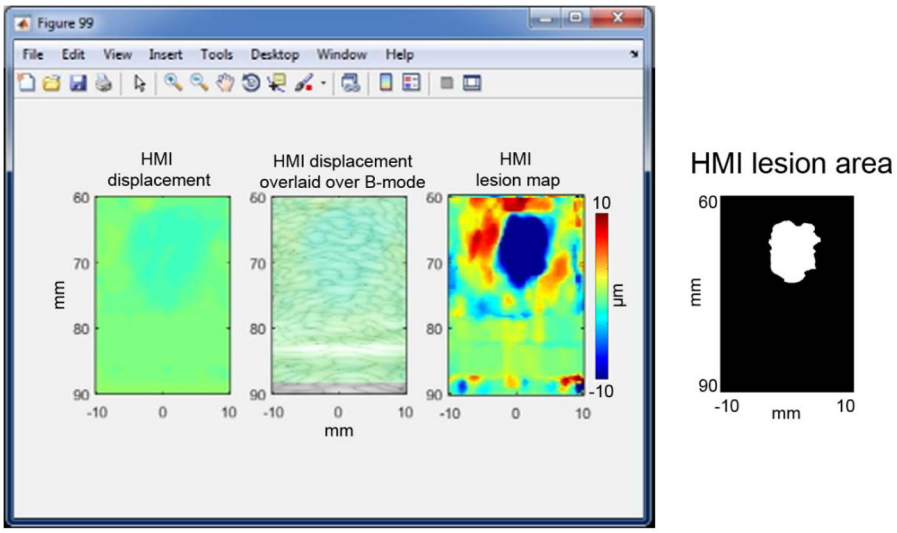

Figure 3.

Real-time HMI displacements. A computer screenshot is shown with the left panel showing real-time HMI displacements. The middle panel shows the filtered HMI displacements overlaid on the B-mode image. A HMI lesion map (right) is shown in the right panel with blue denoting lesion. Corresponding HMI lesion area after −3 dB thresholding is shown on the right side.

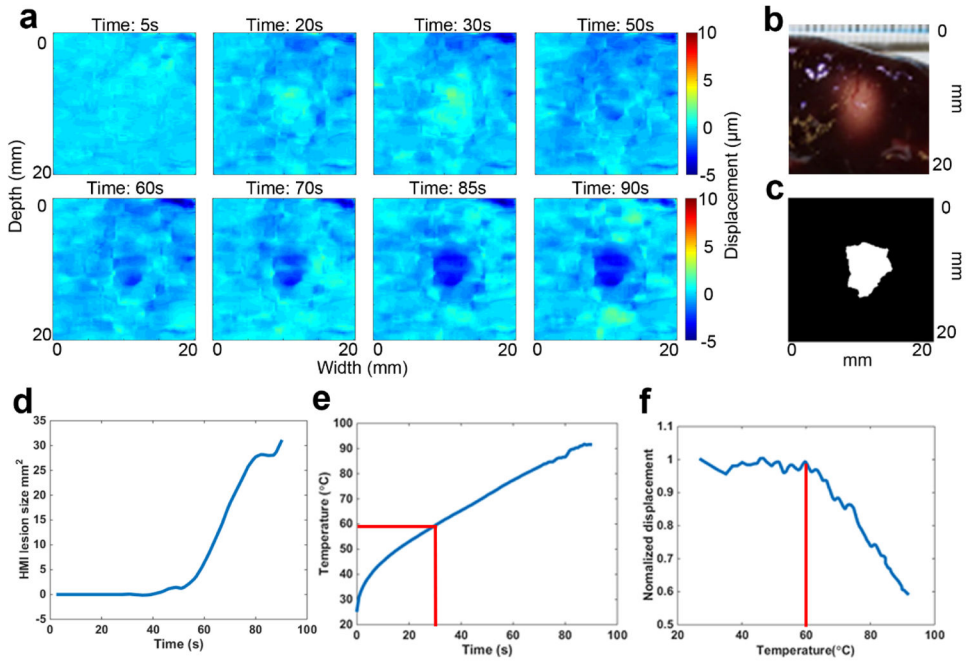

Figure 4.

Example case of HMIgFUS lesion monitoring on 90s ablation. Lesion developing overtime is shown in (a) with blue indicating the formation of the lesion. Gross pathology of the lesion (b) is shown along with the HMI lesion map at the end of ablation (c). (d) HMI lesion size development overtime. (e) Temperature measurement from thermocouple. (f) HMI displacement change during the ablation.

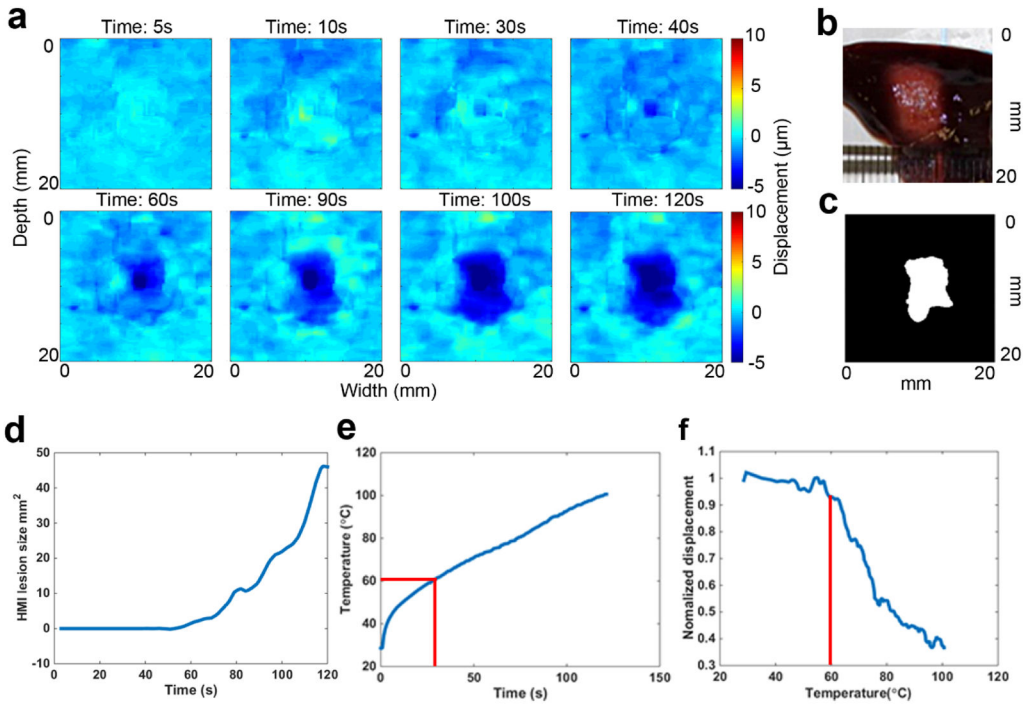

Figure 5.

Example case of HMIgFUS lesion monitoring on 120s ablation. Lesion developing overtime is shown in (a) with blue indicating the formation of the lesion. Gross pathology of the lesion (b) is shown along with the HMI lesion map at the end of ablation (c). (d) HMI lesion size development overtime. (e) Temperature measurement from thermocouple. (f) HMI displacement change during the ablation.

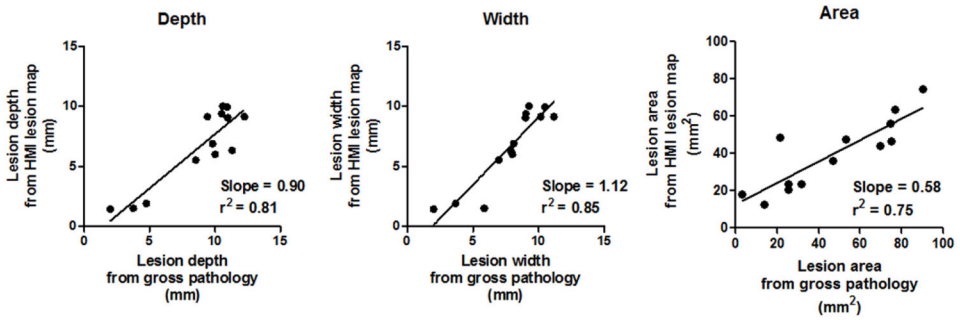

Figure 6.

Lesion dimension comparison between gross pathology and HMI lesion map in depth (left), width (middle) and area (right).

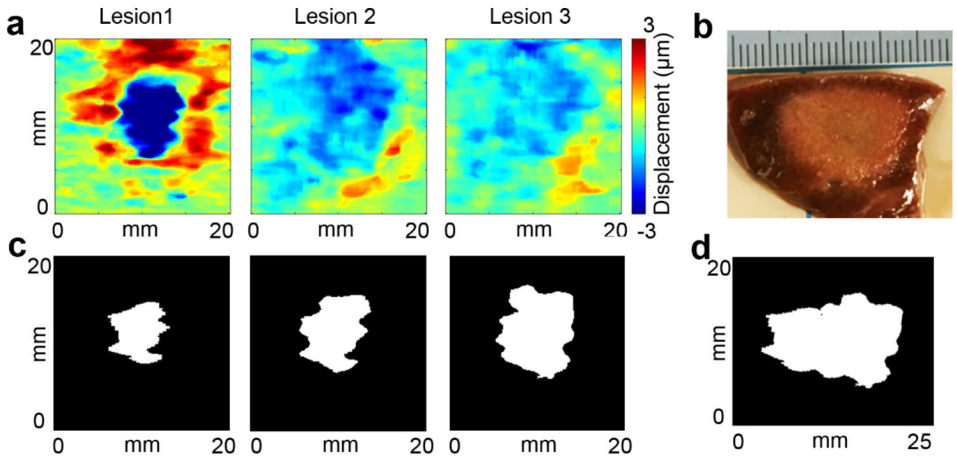

Figure 7.

Multiple-lesion map using HMI in comparison with gross pathology. (a) HMI lesion map at lesion 1, 2 and 3. (b) Lesion gross pathology. (c) HMI lesion map at the end of ablation at lesion 1, 2 and 3. (d) Combined HMI lesion map.

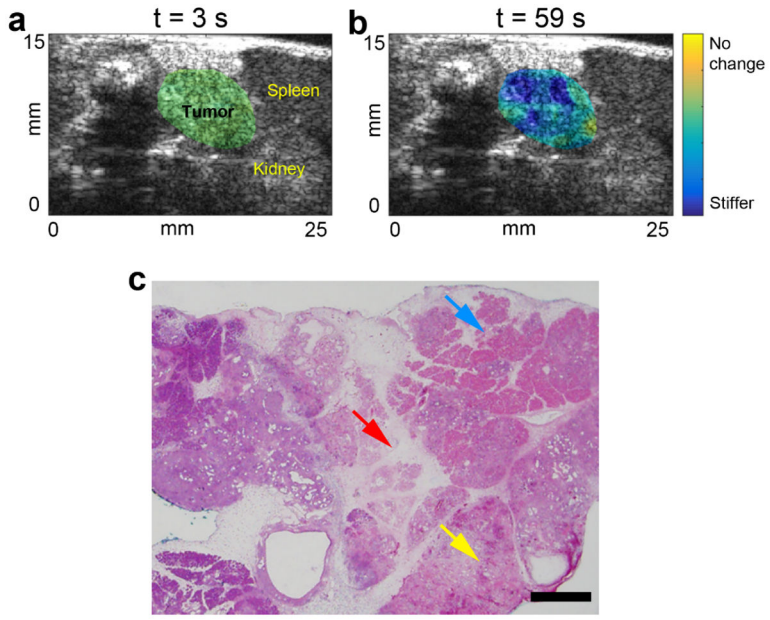

Figure 8.

HMIgFUS lesion formation monitoring in mouse pancreatic tumor. HMIgFUS lesion map at (a) the beginning (t = 3 s) and (b) the end (t = 59 s) of ablation with tumor and adjacent organs marked. (c) H&E stained image of the pancreatic tumor after HIFU ablation show tissue disruption (red arrow), hemorrhaging (yellow arrow) and cell death (blue arrow). The scale bar represents 1 mm.